Supplemental Material

Supplemental Methods

Porcine aortic valve endothelial cell justification and culture

Porcine aortic valve endothelial cells (VEC) are by far the best-characterized and most studied valve endothelial population[1-4]. Non-calcified adult endothelial cells can be obtained from acute traumatic non-cardiac injuries, but are more often acquired from cardiac transplantation surgeries or rejected donor valves. VEC from these sources have a sub-clinical, but likely non-negligible, amount of inflammation and pathology[5-7]. Holliday et al. have shown that human VEC isolated from heart transplant surgeries have elevated α-SMA expression, suggesting some pathobiology may be present, including potentially EndMT[8]. Healthy human VEC have no α–SMA expression *in situ*. Like humans, pigs develop atherosclerotic vascular and valvular lesions without intervention[9,10]. In addition, pigs fed a high fat and cholesterol diet for up to 6 months develop LDL lipid profiles similar to those in humans and form arthelerosclerotic lesions, preferentially on the valve fibrosa, with lipid disposition, calcification, cholesterol clefts, signs of continuous inflammation, and prothrombotic tendency[11-15]. No study to date has demonstrated a pure population of cultured valve endothelial cells from small animals such as mice. Collectively, these findings support the use of porcine valve endothelial cells for the adult valve studies.

Porcine aortic valve endothelial cells were isolated using the method shown by Butcher et al. and Gould and Butcher[1,16]. Porcine heart valves were kindly donated by Shirk Meats of Dundee, NY. Porcine aortic valve endothelial cells (PAVEC) were grown in flasks coated with 50 μg/mL rat tail collagen I (BD Biosciences, San Jose, CA). Cells were cultured at 37^0C and 5% CO_2 in DMEM supplemented with 10% FBS (Invitrogen, Grand Island, NY), 1% penicillin-streptomycin (Invitrogen), and 50 U/mL heparin (Sigma-Aldrich, St. Louis, MO). Culture medium was changed every 48 hours and cells were passaged with 0.05% Trypsin-EDTA (Invitrogen) 1:3 at confluence. Endothelial culture purity was confirmed at the most conservative level via real-time PCR for alpha-smooth muscle actin (not expressed in VEC but expressed in VIC and in cells undergoing EndMT). Cultures with undetectable expression (cycle threshold > 37 cycles) were used in subsequent experiments.

For experiments, 95,000 cells were seeded onto collagen gels at passage 5. After 2 hours 1, 10, or 100 ng/mL of human IL-6 (Sigma-Aldrich) or human TNF-α (Sigma-Aldrich) was added to the culture medium for treated cells. For IL-6 inhibitor experiments seeded cells were allowed to attach for 2 hours before the addition of 100 ng/mL IL-6 and 5 μm Akt Inhibitor XI (EMD Chemicals, Gibbstown, New Jersey) or 25 μm STAT3 Inhibitor Peptide (EMD Chemicals). In TNF-α inhibitor experiments 100 ng/mL TNF-α with 5 μm Akt Inhibitor XI, 25 μm MEK1 inhibitor PD 98059 (EMD Chemicals), or 10 μm SB 431542 ALK5 inhibitor (Sigma-Aldrich) was added to cultures. After 48 hours cell invasion was quantified manually at 60 μm depth into the gel (see Supplementary Figure I). Immediately after quantifying cell invasion cells were fixed for immunofluorescence in 4% paraformaldehyde or processed for RNA isolation.

Avian endocardial explant culture

The embryonic avian (chick and quail) is a standard animal model for understanding heart and valve development and is ideal for these studies. The avian (quail, chick) embryo does not require a placental circulation and can be cultured outside of the egg for almost all of its gestation[17,18] therefore not requiring death of the mother. Though there are some differences in cardiac anatomy between avians and mammals, the morphogenesis, remodeling, and final anatomy of the clinically important left side of the heart is remarkably similar between chicks and humans[19-22]. Late fetal and postnatal avian aortic and mitral valves exhibit well developed

trilaminar matrix striation and fibroblastic cell phenotype similar to humans, whereas matrix stratification is barely detectable in mice[19]. Biological assays with avian and mouse valve progenitors demonstrate identical molecular mechanisms and participants (though specific isoforms may differ)[23,24]. As each assay we perform pools multiple explants per sample, conducting similar experiments with mice would require an impractical number of identically timed pregnant females. The avian is the only embryo model that enables isolation of sufficient numbers of valve explants for 3D *in vitro* experimentation, and therefore suitable for the embryonic experiments. We utilize the chick for its sequenced genome (enabling PCR design), and quail for its QH1 antigen identifying endocardial cells.

Fertile quail eggs were acquired from Lake Cumberland Game Bird Farm (Monticello, KY). Eggs were incubated at 37°C and 60% humidity to stage HH14^{-}. The embryos were placed into sterile Earl's Basic Salt Solution (EBSS, Invitrogen) and staged according to the criteria of Hamburger and Hamilton[25]. Quail endocardial explant isolation has been previously described[26]. Following endocardial cell isolation, M199 was added to the wells containing 1, 10, or 100 ng/mL of human IL-6 or human TNF-α. For inhibitor experiments 100 ng/mL IL-6 was added with 5 μm Akt Inhibitor XI, 25 μm STAT3 Inhibitor Peptide, or 10 μm SB 431542 ALK5 inhibitor or 100 ng/mL TNF-α was added with 5 μm Akt Inhibitor XI, 25 μm MEKK1 inhibitor PD 98059, or 10 μm SB 431542 ALK5 inhibitor. Cell invasion was quantified manually at a 60 µm depth into the gel after 48 hours (see Supplementary Figure I). The cultures were then fixed in 4% paraformaldehyde for immunofluorescence or processed for RNA isolation.

Three dimensional collagen constructs

Three dimensional collagen gels at a concentration of 1.5 mg/mL collagen were made by combining ice-cold 3X Dulbecco's Modified Eagle's Medium (DMEM, PAVEC; Invitrogen, Carlsbad, CA) or 3X M199 (QEE, Invitrogen), 10% Fetal Bovine Serum (FBS, PAVEC; Invitrogen) or 1% Chick Serum (CS, QEE; Invitrogen), sterile 18 MΩ water, 0.1 M NaOH, and rat tail collagen I (BD Biosciences). A 0.3 mL aliquot of the collagen solution was pipetted into 4 well tissue culture plates (1.9 cm^2 growth area; Nunc, Rochester, NY) and allowed to gel for at least 1 hour at 37^{o}C and 5% CO_2.

Collagen gel immunofluorescence

Fixed samples on collagen gels were washed for 15 minutes on a rocker 3 times with PBS, permeabilized with 0.2% Triton-X 100 (VWR International, West Chester, PA) for 10 minutes, and washed another 3 times with PBS. Samples were incubated overnight at 4^{o}C in a 1% BSA (Rockland Immunochemicals, Inc., Gilbertsville, PA) blocking solution followed by another 4^{o}C overnight incubation with mouse anti-porcine PECAM 1:100 (AbD Serotech, Raleigh, NC), rat anti-porcine VE-cadherin 1:100 (AbD Serotech), or mouse anti-quail QH1 (DSHB, Iowa City, Iowa) and rabbit anti-human α-SMA 1:100 (Spring Bioscience, Pleasanton, CA). For NFκB staining, samples were incubated with rabbit anti-human NFκB p105 / p50 1:100 (Abcam, Cambridge, MA). For pSMAD staining, samples were incubated with pSMAD2 rabbit anti-human 1:50 (Cell Signaling Technology, Beverly, MA). After 3 washes for 15 minutes with PBS, samples were exposed to Alexa Fluor® 488 or 568 conjugated (Invitrogen), species specific secondary antibodies at 1:100 in 1% BSA for 2 hours at room temperature. Three more washes with PBS for 15 minutes were followed by incubation with DRAQ5 far red nuclear stain (Enzo Life Sciences AG, Lausen, Switzerland) at 1:1000. Samples were washed once more with 18 MΩ water and stored in 18 MΩ water at 4^{0}C. Images were taken with a Leica TCS SP2 (Exton, PA) or Zeiss 710 (Thornwood, NY) laser scanning confocal microscope. NFκB and pSMAD2/3 nuclear co-localization was measured with Metamorph 7.1 software (Molecular Devices). Green (NFκB) and far red (nuclei) channels were each thresholded. Regions were

created around each nuclei. The regions were transferred onto the green channel and the thresholded stained area was quantified within the regions.

Human valve section immunofluorescence

Diseased human aortic valves were obtained from adults undergoing planned, non-elective valve replacement surgery by Dr. Sanjay Samy at Robert Packer Hospital in Sayer, PA. Pediatric valves were obtained from Dr. Jonathan Chen, Cornell-Weill Medical School and NY Presbyterian Hospital. Fixed human valves were paraffin embedded and sectioned at 6 μm. Sections were placed on slides, de-waxed, hydrated, and antigens were retrieved by placing the slides in 10 mM TRIS base buffer at pH 10.0 at 90°C for 40 minutes. Following antigen retrieval sections were washed with PBS, permeabilized with 0.1% Tween-20, washed again with PBS, and blocked for 1 hour with 5% BSA in PBS. Primary antibodies were added at a concentration of 1:100 and incubated overnight at 4°C. The following primary antibodies were used: human anti-mouse P2B1 (DSHB), rat anti-porcine VE-cadherin (AbD Serotech), rabbit anti-human α-SMA (Spring Bioscience), rabbit anti-human NFκB p105 / p50 (Abcam), and anti-human Cy5.5-labelled CD45 (generously provided by Dr. Michael King, Department of Biomedical Engineering, Cornell University, Ithaca, NY). Sections were incubated with species-specific secondary antibodies at 1:100 for 1 hour, washed with PBS, incubated with 1:1000 DRAQ5 (Enzo Life Sciences AG) or 2:10,000 Hoechst 33342 (Invitrogen) for 30 minutes, washed again with PBS, mounted with Prolong Gold antifade reagent (Invitrogen), and imaged with a confocal microscope.

Western blots

P4 PAVEC and PAEC were grown to 70% confluency in a 6-well plate and treated with culture medium alone, 100 ng/mL TNF-α, or 100 ng/mL TGFβ-1 for 48 hours at 37°C. Cells were lysed directly on the plate using RIPA buffer supplemented with 25mM NaF, 1mM NaVO4, and 0.5% protease inhibitor cocktail (Sigma-Aldrich), incubated for 15 min at RT, scraped and homogenized by pipetting up and down, and centrifuged at 15,000 rpm for 10 min. 10ug of protein was loaded into a 10% gel with Laemmli buffer at 1:1 ratio and run for 1 hour at 120V in 25mM Tris, 0.2M Glycine, 1% SDS running buffer. Western blot transfer to nitrocellulose membrane (Thermo Scientific, Rockford, IL) was performed at 400mA for 1 hour in 25mM Tris, 20% methanol transfer buffer. After rinsing in PBS with 0.1% Tween-20, the membrane was blocked for 1 hour in Odyssey Blocking Buffer at RT. Mouse anti-pig CD31 (Springer Bioscience, 1:1000), mouse anti-human VE-cadherin (Abcam, 1:500), rabbit anti-human alpha-smooth muscle actin (Abcam, 1:1000), rabbit anti-human Smad2 and pSmad2 (Cell Signaling, 1:2000), rabbit anti-Snai1 (SCBT, 1:200), and mouse anti-human GAPDH (Ambion, 1:2000) were used in Odyssey blocking buffer+0.1%Tween-20 to detect protein expression. The membrane was washed 4x in PBS-tween, 1X in PBS, and incubated overnight at 4°C with gentle agitation. The same washes were then performed and the membrane was incubated in Odyssey blocking buffer +0.1% Tween-20, +0.2% SDS with 1:20,000 anti-mouse and anti-goat secondary antibodies (Li-Cor IRDye). Blots were imaged using the Odyssey Infrared system (Li-Cor).

RT-PCR

Total RNA was extracted using a Norgen total RNA purification kit (Norgen Biotek Corp., Thorold, ON) and RNA was reverse transcribed to cDNA using the SuperScript III RT-PCR kit with oligo(dT) primer (Invitrogen). RT-PCR was performed on all samples using SYBR Green PCR master mix (Applied Biosystems, Foster City, CA) and a MiniOpticon Real-Time PCR Detection System (Biorad, Hercules, CA). Primer sequences are listed in Supplementary Table S1.

Apoptosis Assay

Fixed samples on collagen gels were examined for apoptosis using the APO-Brdu TUNEL assay (Invitrogen) according to the instructions provided by the manufacturer. Briefly, the samples were washed 3 times in the wash buffer and then incubated in DNA labeling solution for 2 hours at 37^{o}C. Samples were washed for 5 minutes on a rocker with rinse buffer, then incubated in Anti-BrdU mouse monoclonal antibody PRB-1, Alexa Fluor 488 conjugate 1:50 (Invitrogen) and Draq5 1:1000 (Enzo Life Sciences AG) for 1 hour at room temperature. 200uL of propidium iodide stain was added to each sample and then incubated for 30 minutes at room temperature. Samples were stored in PBS at 4^{o}C and imaged less than 24 hours later. Images were taken with a Zeiss 710 laser scanning spectral confocal microscope. Custom Matlab code was used to threshold the red (propidium iodide), green (Brdu labeling) and far red (nuclei) channels according to the automated global thresholding level given in analysis of the far red channel. Cell boundaries, nuclei, and Brdu labeling were confirmed visually for each sample. Numbers of apoptotic cells per sample were counted via Matlab using Brdu labeling within a cell boundary as the criteria for identifying an apoptotic cell.

Proliferation Assay

Brdu labeling reagent (Invitrogen) was added to PAVEC culture medium 6 hours prior to experiment completion. At 48 hours cells were fixed as described above and processed in the same manner as the apoptosis assay. Brdu labeling within a cell nucleus was the criteria for a proliferating cell.

Statistics

Results are expressed as mean ± standard error, $n \geq 3$. Data was analyzed with GraphPad Prism version 4.00 for Windows (GraphPad Software, San Diego, CA). An unpaired student's t-test or a one-way ANOVA with Tukey's post test was used to compare differences between means and data was transformed when necessary to obtain equal sample variances. Differences between means were considered significant at $p < 0.05$.

Supplemental Table

Table I. Primer sequences

Primer	**Forward sequence**	**Reverse sequence**
Pig 18S	aatggggttcaacgggttac	tagagggacaagtggcgttc
Pig ACTA2	cagccaggatgtgtgaagaa	tcacccccctgatgtctagga
Pig PECAM1	atctgcatctcgtgggaagt	gagctgaagtgtcagcagga
Pig Snail	gcccaactacagcgagctac	ccaggagagagtcccagatg
Pig TGFB1	ccactctcagcctctctgct	tgggttctcggtatcctacg
Pig VCAM1	ttgtttcctcgtcacacagc	caatctgcgcaatcattttg
Pig ICAM1	aaaggaggctccatgaaggt	tgccatcgttttccacatta
Pig AKT1	ggcaggaggaagagatgatg	cccagcagcttcaggtactc
Pig MEK1	gagagccgatttgaagcaac	actctgccacttcccaaatg
Pig NFKB1	aggatgggatctgcactgtc	atcagggtgcaccaaaagtc
Chick 18S	cggagagggagcctgagaa	cgccagctcgatcccaaga
Chick ACTA2	cagttttcccttccatcgtg	tggggtatttcaaggtcagg
Chick PECAM1	tcactccagtggcatgaaaa	gccaagatccttcttccaca
Chick Slug	cctcctccaaagatcacagc	ccaacccagagaaagtggaa
Chick TGFB3	ggcttgtacaacacgctgaa	tgcaggatttcaccaccata
Chick VCAM1	attcctcatgcccatttcac	ctgaactcgatgggaaaacc
Chick ICAM1	tggccagaaacatatccaca	gcagttccaagattggcttc
Chick AKT1	gatggcacattcattggcta	ggtccactggaggcatctaa
Chick MEK1	aaaccagatcatccgtgagc	tccagccttttcagcactt
Chick NFKB1	atccccaaatgtttgcaatg	tcgaaaacccctctgttttg
Chick IL6RA	ctatggatgaagcgcaggtt	gacaccacgagggctttg
Chick TNFRSF1A	cagtgatgcagtttgcaggt	aggttcccattcagctcaga

Supplemental Figures and Figure Legends

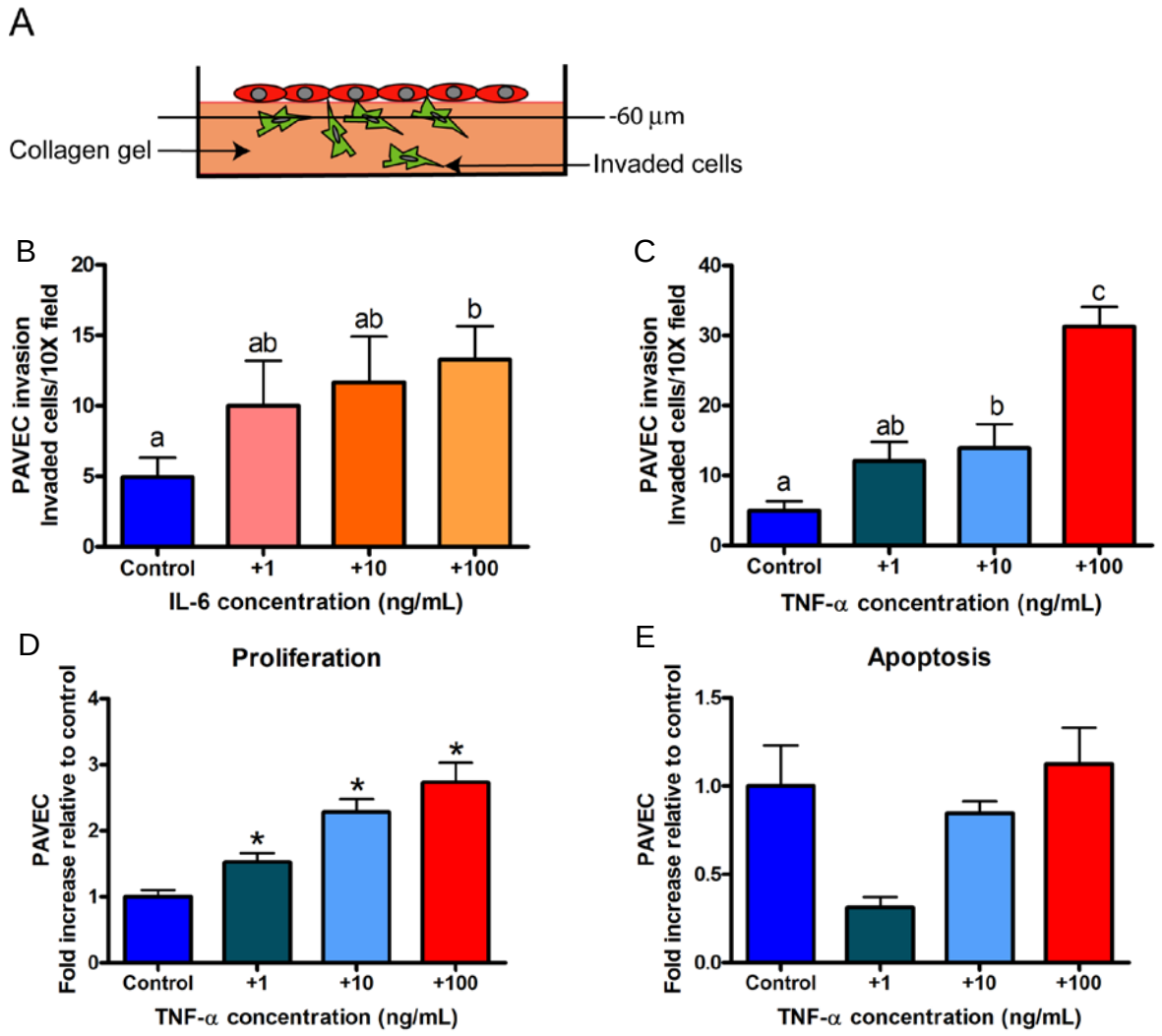

Figure I. (A) Cell invasion assay. Embryonic valve endocardial or adult valve endothelial cells are plated onto a 3D collagen gel. After 48 hours, invaded, mesenchymally transformed cells are quantified using a 10X objective and an inverted microscope. First the microscope is focused on the endocardial or endothelial layer on the surface of the gel. Next the microscope is focused 60 μm down into the gel, and the number of in-focus invaded cells is quantified. This process is repeated for all endocardial explants present on the gel, or for four fields in the center of the gel for endothelial monolayers. (B-E) Inflammatory cytokine dose response, proliferation and apoptosis in porcine aortic valve endothelial cells (PAVEC). (B) 100 ng/mL IL-6 treatment for 48 hours significantly increases cell invasion when compared with controls. (C) A 48 hour 100 ng/mL TNF-α treatment significantly increases cell invasion when compared with control, +1 ng/mL, and +10 ng/mL treatments. PAVEC showed a significant increase in proliferation (D), but not apoptosis (E), in response to increasing doses of TNF-α for 48 hours. Error bars show ±SEM, n ≥ 3 independent monolayers. Bars that do not share any letters are significantly different according to a one-way ANOVA with Tukey's post test ($p \leq 0.05$).

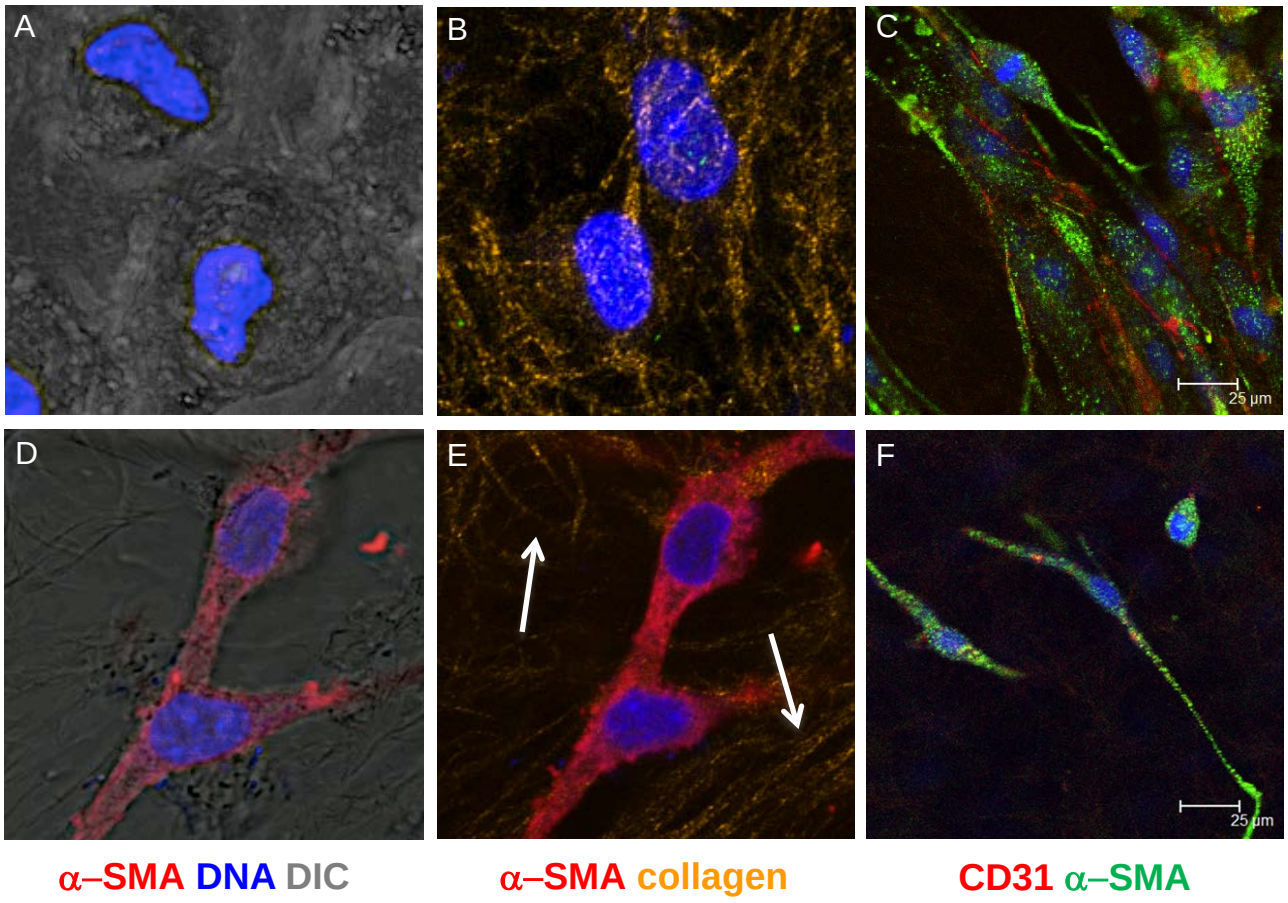

Figure II. Exposure to inflammatory cytokines induces mesenchymal transformation and invasion in adult endothelial cells. Confocal images of control porcine aortic valve endothelial cells (PAVEC) 48 hours after plating at the surface of the 3D collagen gel (A, B). PAVEC 48 hours following exposure to 100 ng/mL TNF-α (D, E). PAVEC 48 hours following exposure to 100 ng/mL TNF-α at the surface of the gel (C) and -60 μm into the gel (F), cells co-express CD31 and α-SMA. Arrows show collagen fiber arrangement, invaded cells exposed to TNF-α remodel collagen fibers.

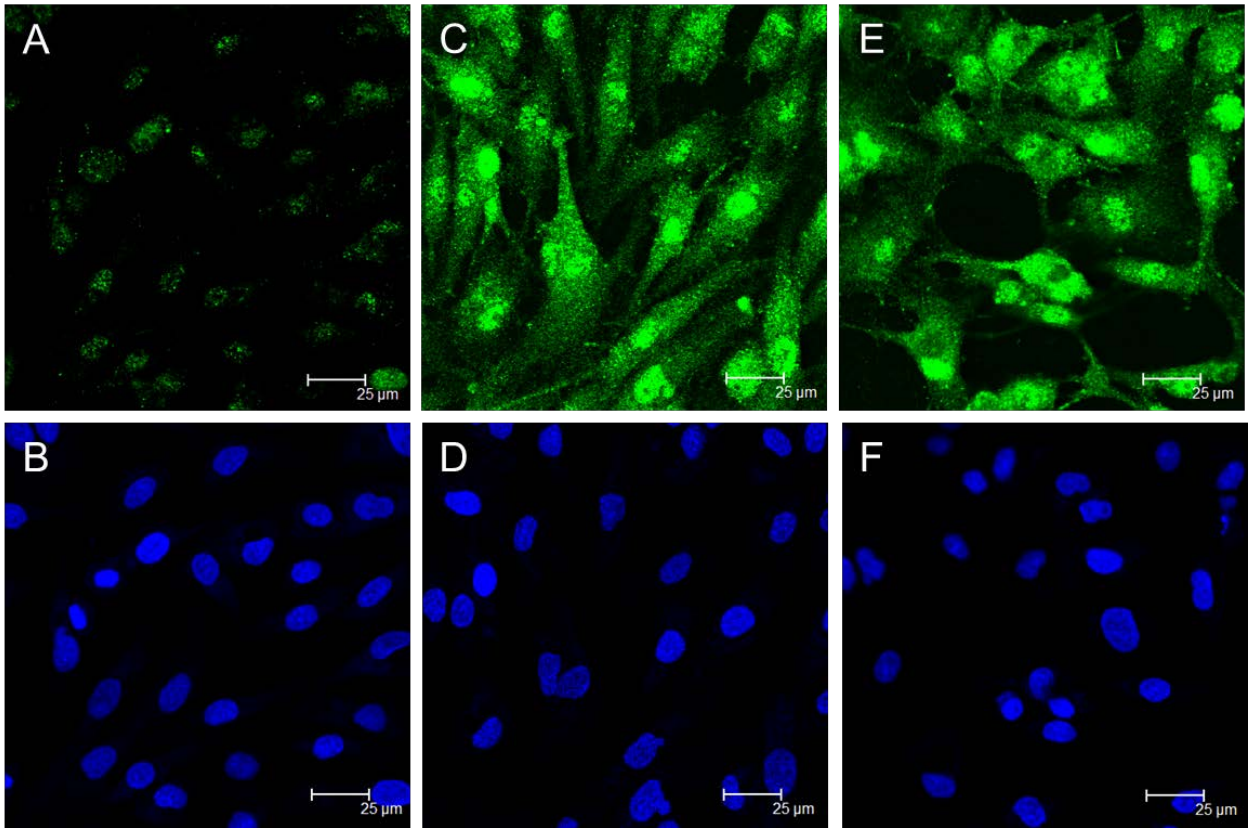

Figure III. Separate green and blue channels for confocal images of control (A, B), +100 ng/mL IL-6 (C, D), and +100 ng/mL TNF-α (E, F) PAVEC at a 48 hour time point stained for NFκB (green) and DNA (blue).

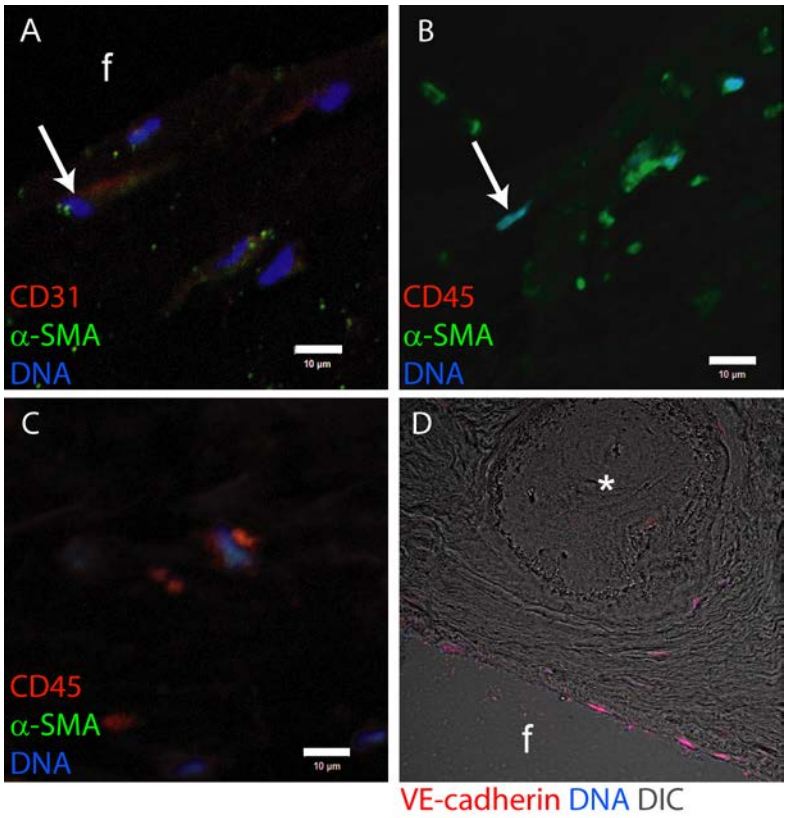

Figure IV. Diseased human aortic valve immunohistochemistry. A, B) Human aortic valve endothelial cells co-expressing CD31 and α-SMA do not also express CD45, an immune cell marker. Arrows show the same cell in consecutive sections co-expressing CD31 and α-SMA, but not expressing CD45. C) CD45-positive immune cells are present in the diseased human valve. D) The endothelium near the nodule (*) is degraded, and VE-cadherin expression is decreased. Scale bar = 10 μm.

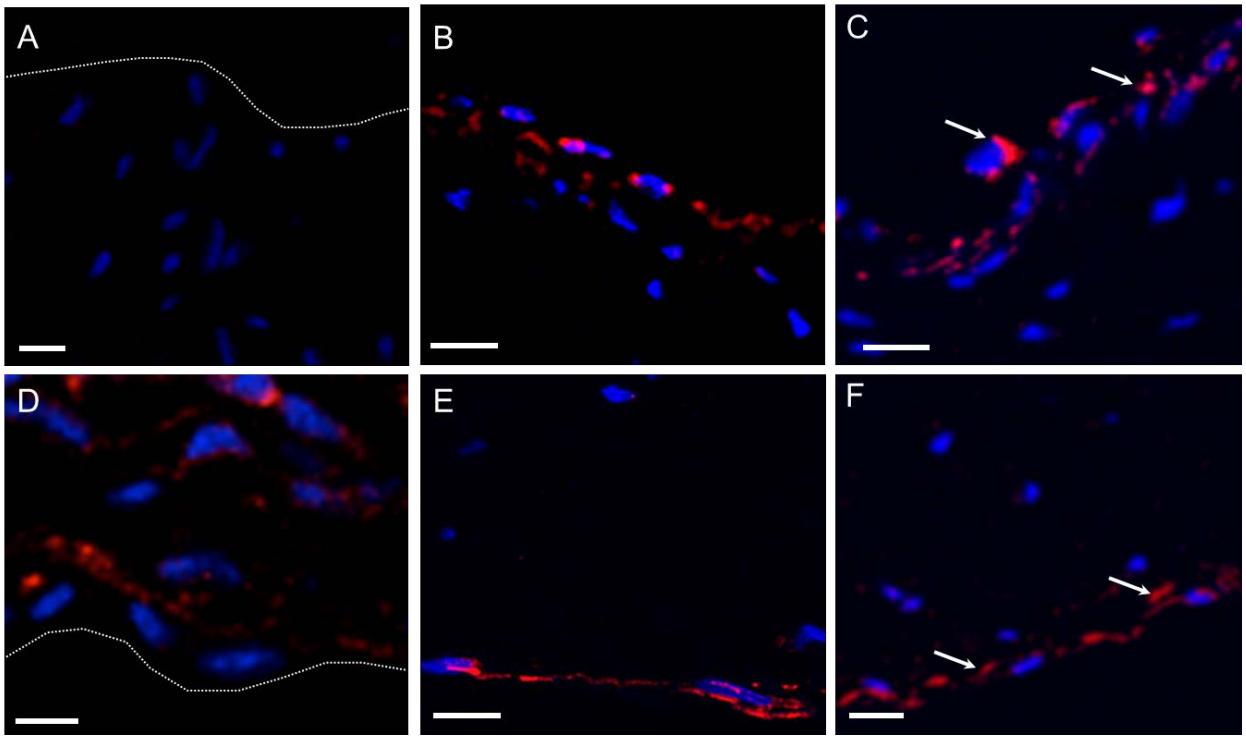

Figure V. Healthy human pediatric valve immunohistochemistry. Healthy human aortic valve endothelial cells do not co-express VE-cadherin and α-SMA and do not express nuclear NFκB. A-C) fibrosa, D-F) ventricularis. A,D) α–SMA. B,E) VE-cadherin. C,F) NFκB, arrows show lack of nuclear staining in fibrosa and ventricularis endothelial cells. Scale bar = 10μm.

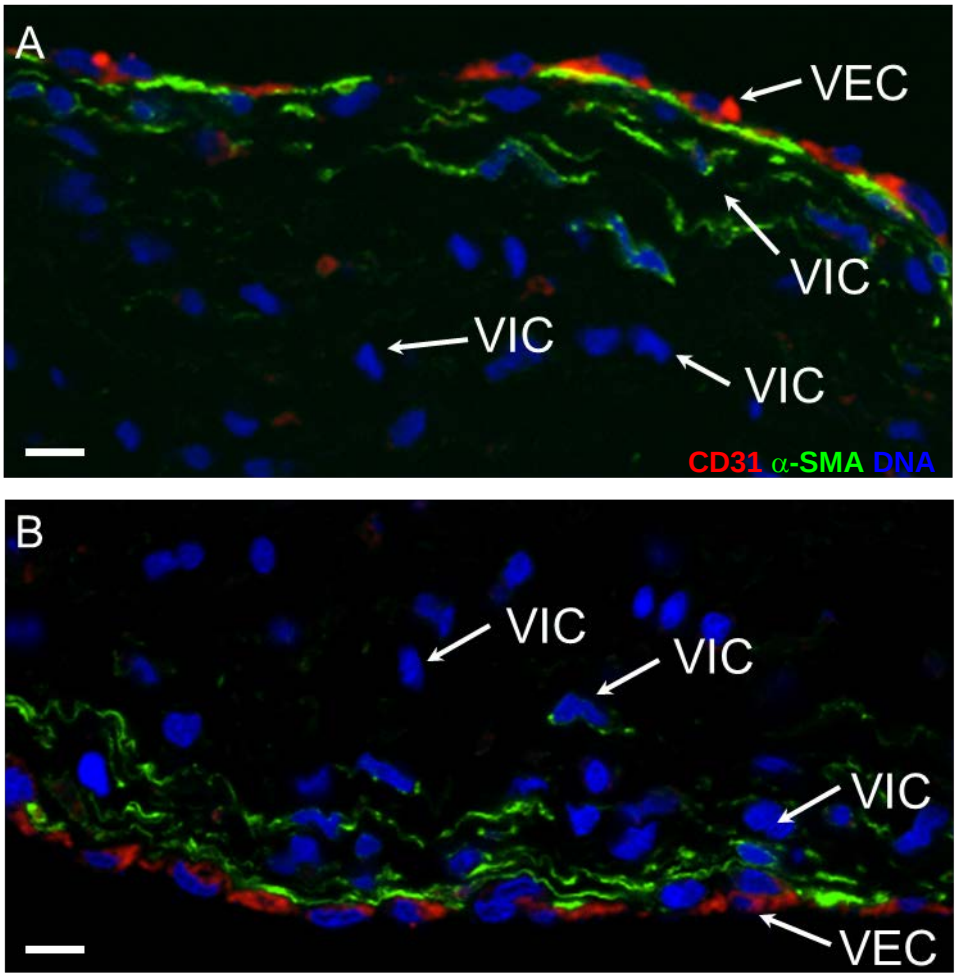

Figure VI. Healthy human pediatric valve. A) fibrosa, B) ventricularis. Green: α–SMA, red: CD31, blue: DNA. Scale bar = 10μm.

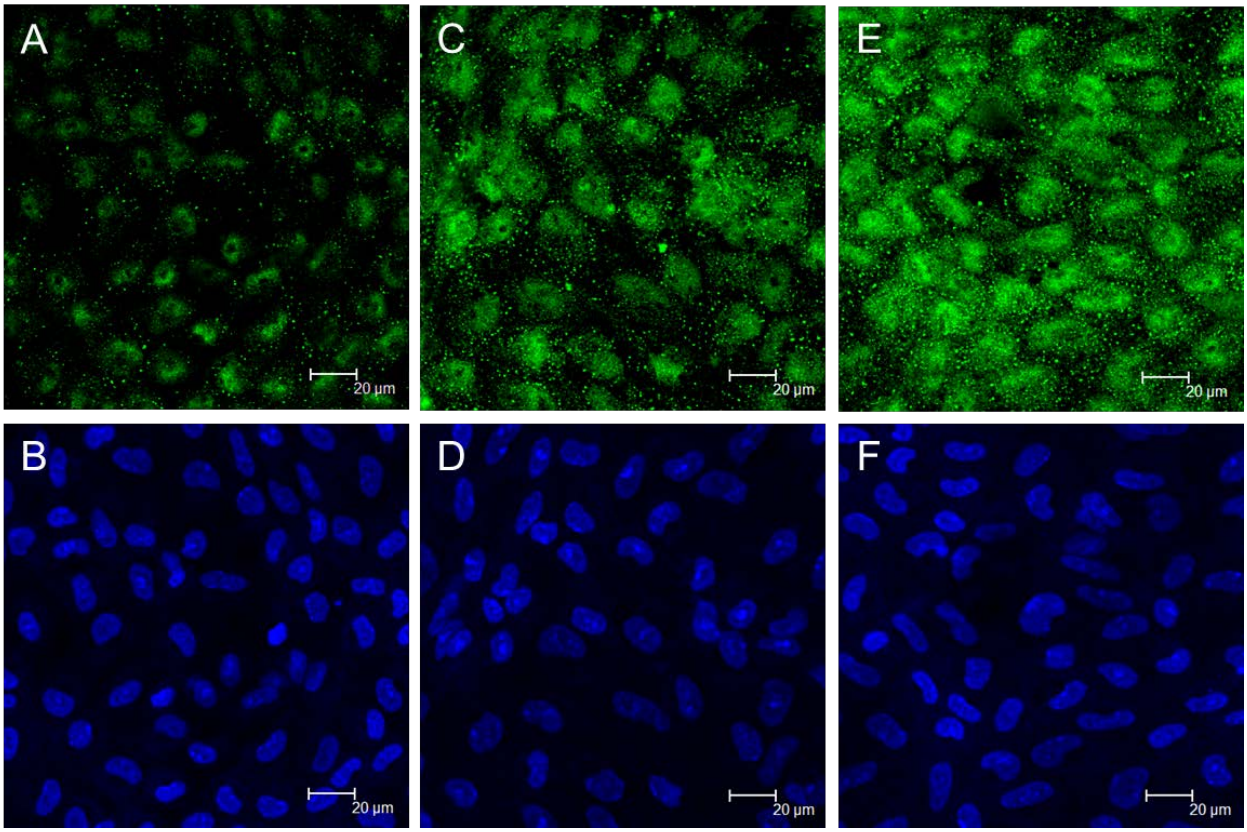

Figure VII. Separate green and blue channels for confocal images of control (A, B), +100 ng/mL IL-6 (C, D), and +100 ng/mL TNF-α (E, F) QEE at a 48 hour time point stained for NFκB (green) and DNA (blue).

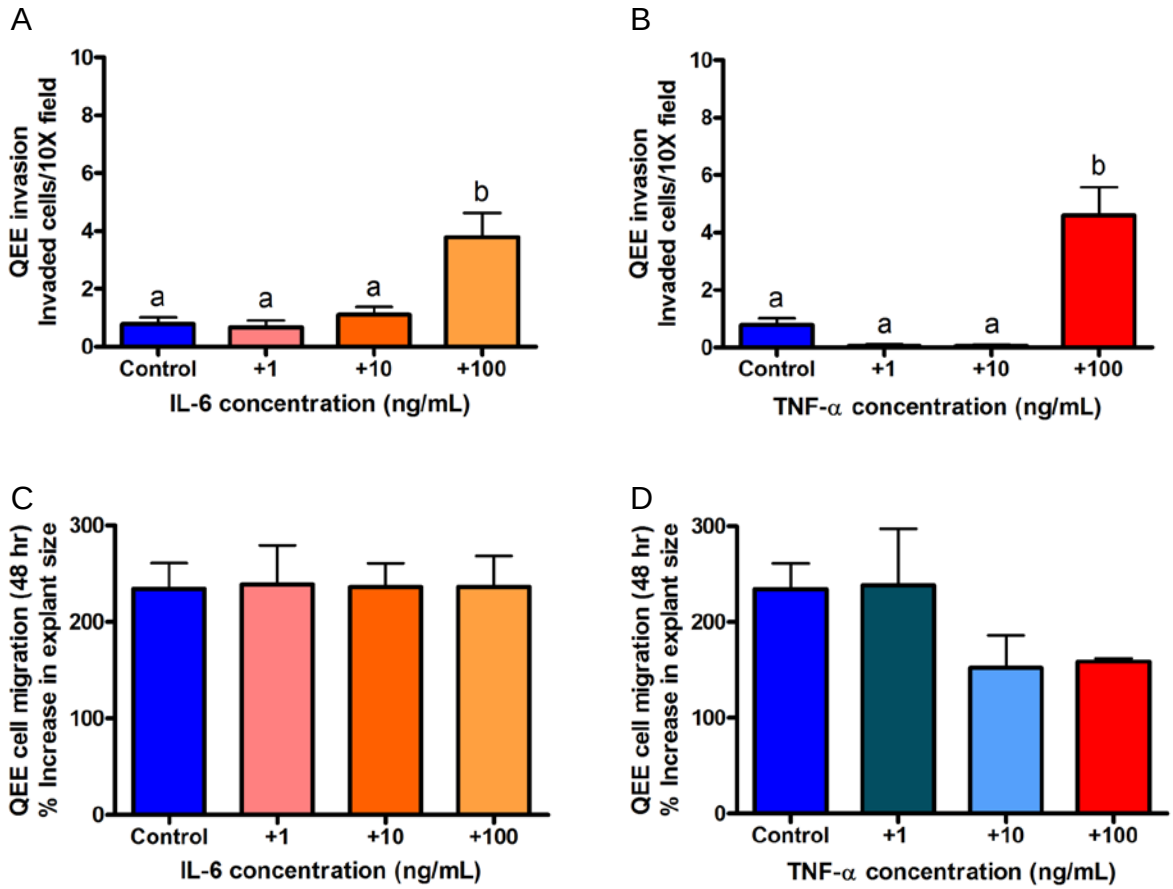

Figure VIII. Inflammatory cytokine dose response migration and proliferation in quail endocardial explants (QEE). A, B) A 48 hour exposure to 100 ng/mL IL-6 or TNF-α significantly increases cell invasion when compared with control, +1 ng/mL, and +10 ng/mL treatments. C,D) QEE size increased by ~250% after 48 hours, cytokine exposure had no significant effect of QEE proliferation. Error bars show ±SEM, n ≥ 3 batches of pooled explants (QEE). Bars that do not share any letters are significantly different according to a one-way ANOVA with Tukey's post test ($p \leq 0.05$).

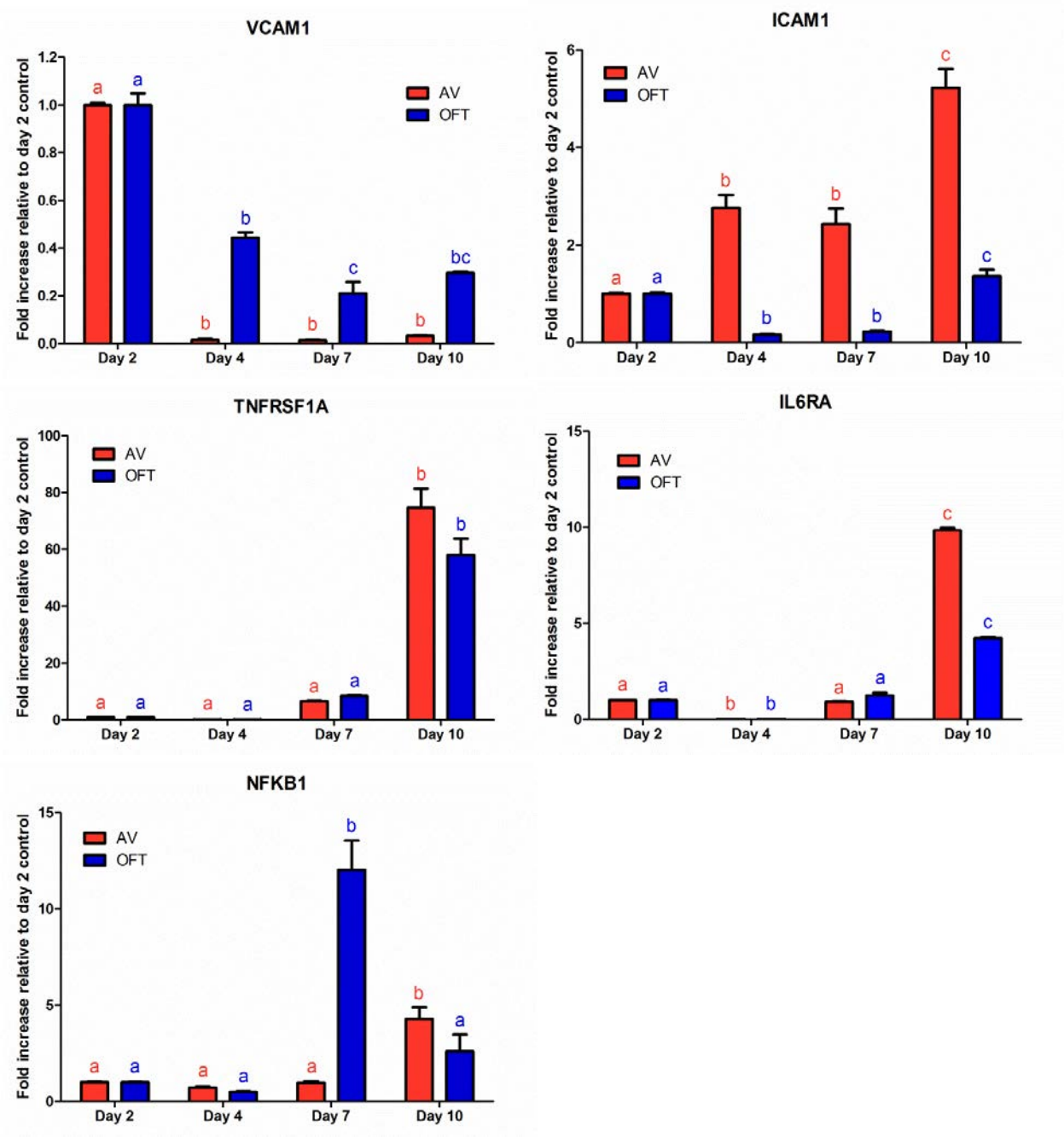

Figure IX. Inflammatory gene expression in embryonic valve forming regions. VCAM1, ICAM1, TNFRSF1A (the gene that codes for TNFR1), IL6RA (the gene that codes for IL-6Rα), and NFKB1 in chick day 4, day 7, and day 10 atrioventricular (AV) cushions or valves and outflow tracts (OFT) normalized to day 2 chick AV or OFT. Error bars show ±SEM, n ≥ 3. Bars that do not share any letters are significantly different according to a one-way ANOVA with Tukey's post test ($p \leq 0.05$).

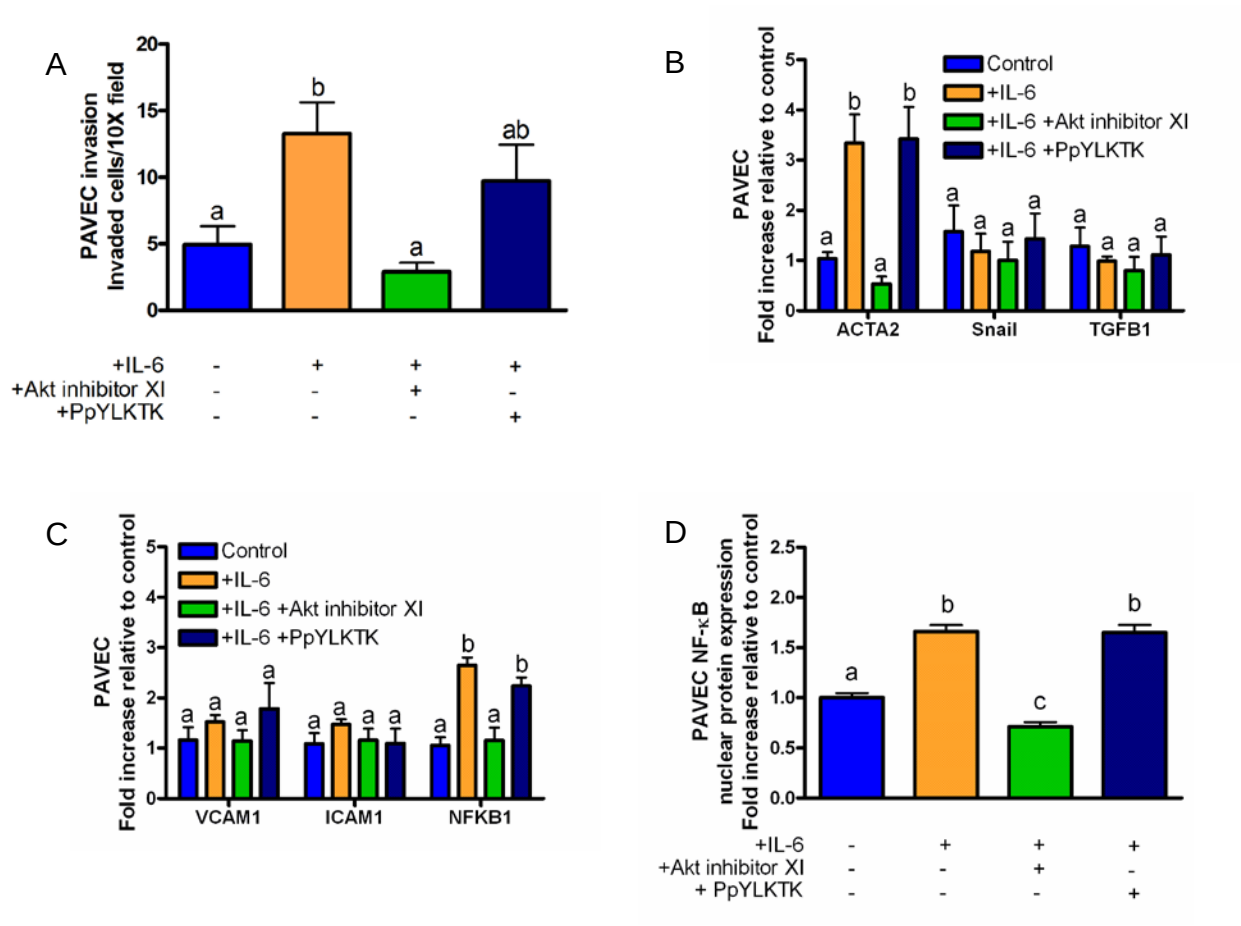

Figure X. Inflammatory cytokines induce EndMT through Akt/NFκB in PAVEC. A) Cell invasion after to exposure to 100 ng/mL IL-6 or 100 ng/mL IL-6 with 5 μm Akt inhibitor XI or 5 μm PpYLKTK STAT3 inhibitor. B) ENDMT-related gene expression after exposure to 100 ng/mL IL-6 with inhibitors. C) Inflammatory activation-related genes after exposure to 100 ng/mL IL-6 with inhibitors. D) PAVEC nuclear factor kappa b (NFκB) nuclear localization quantification after exposure to 100 ng/mL IL-6 with inhibitors. Error bars show ±SEM, n ≥ 3 independent monolayers. Bars that do not share any letters are significantly different according to a one-way ANOVA with Tukey's post test ($p \leq 0.05$).

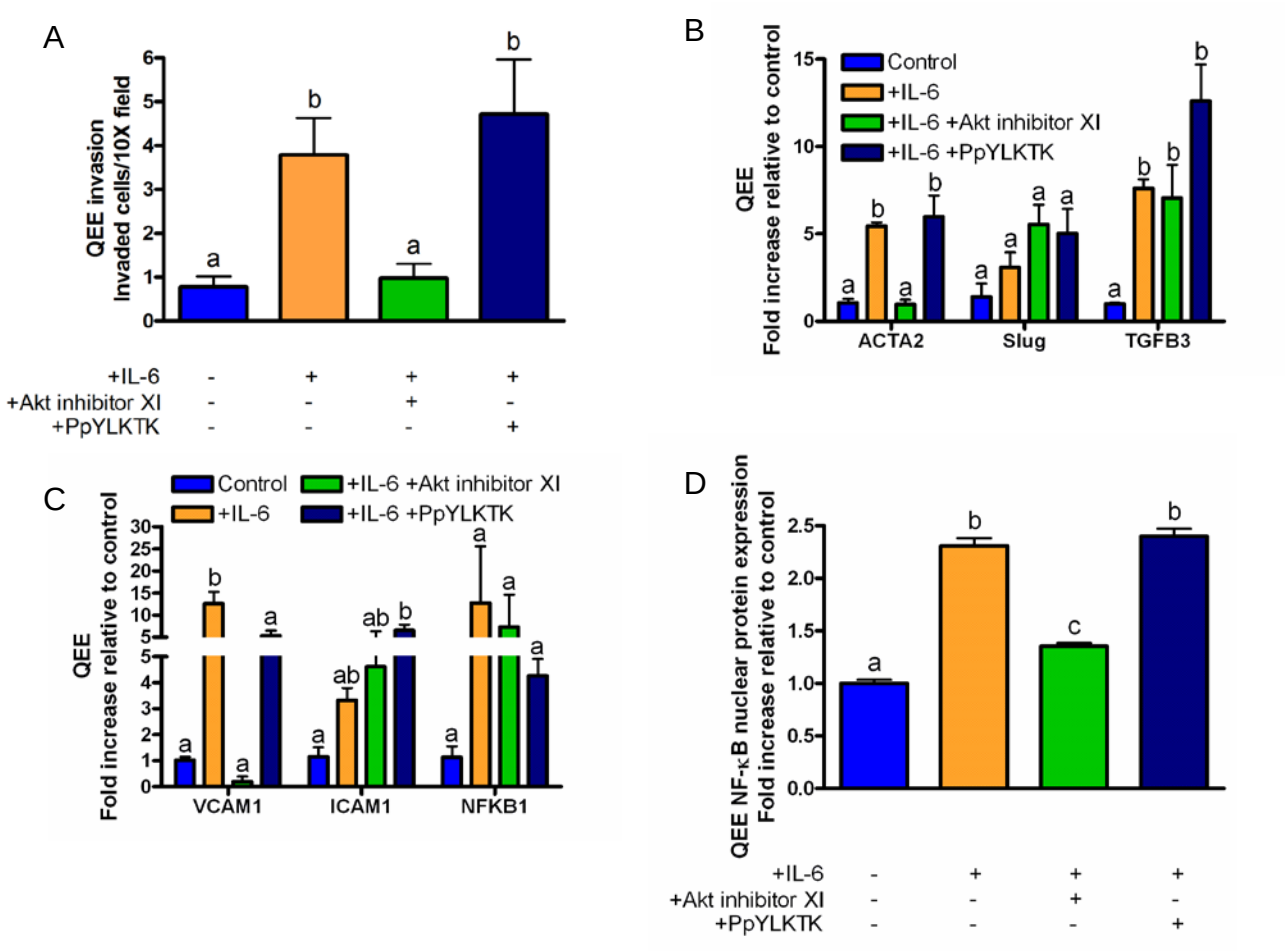

Figure XI. Inflammatory cytokines induce EndMT through Akt/NFκB in QEE. A) Cell invasion after to exposure to 100 ng/mL IL-6 or 100 ng/mL IL-6 with 5 μm Akt inhibitor XI or 5 μm PpYLKTK STAT3 inhibitor. B) EndMT-related gene expression after exposure to 100 ng/mL IL-6 with inhibitors. C) Inflammatory activation-related genes after exposure to 100 ng/mL IL-6 with inhibitors. D) QEE nuclear factor kappa b (NFκB) nuclear localization quantification after exposure to 100 ng/mL IL-6 with inhibitors. Error bars show ±SEM, n ≥ 3 batches of pooled explants. Bars that do not share any letters are significantly different according to a one-way ANOVA with Tukey's post test ($p \leq 0.05$).

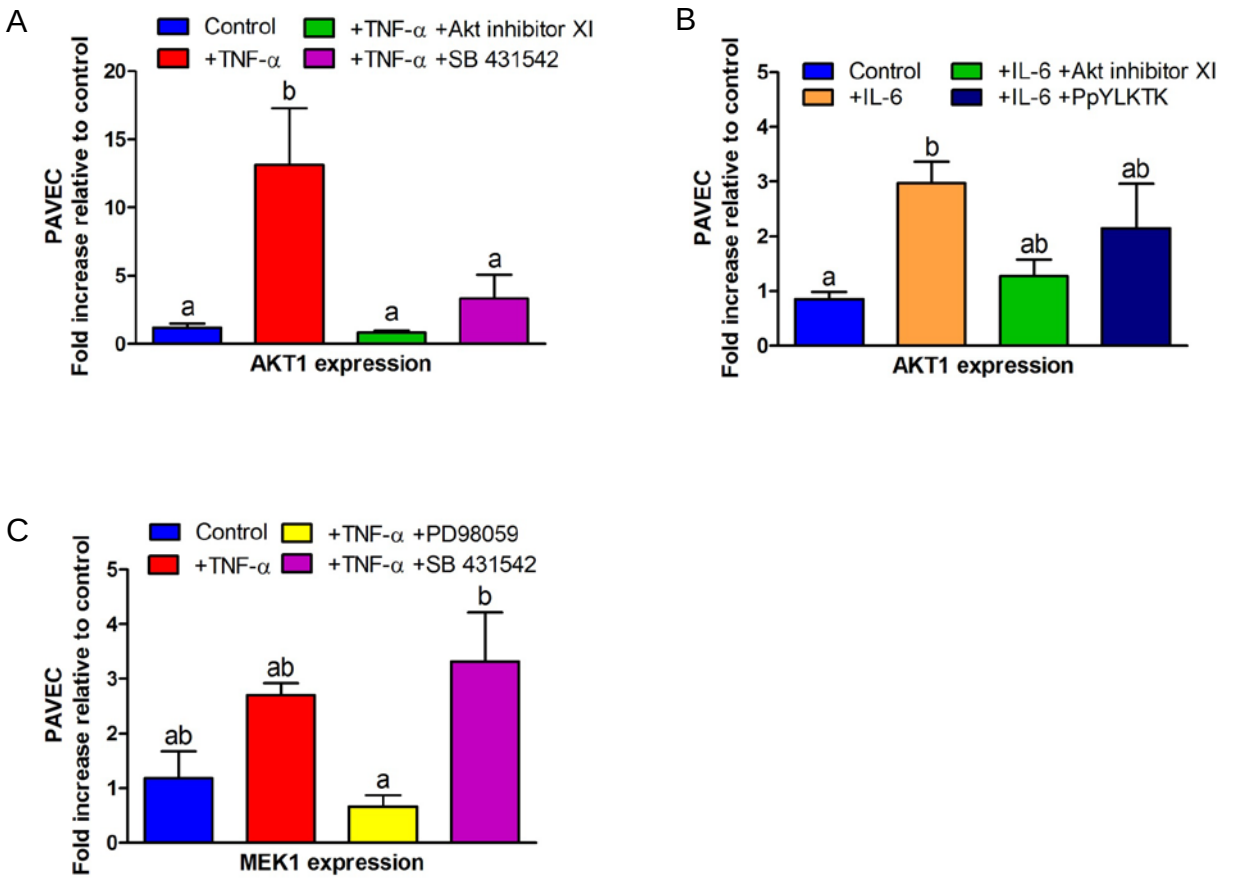

Figure XII. AKT1 gene expression was blocked by Akt inhibition and MEK1 gene expression was blocked by MEK1 inhibition in PAVEC. A) AKT1 expression was blocked in PAVEC following exposure to 100 ng/mL TNF-α and 5 μm Akt inhibitor XI. B) AKT1 expression was blocked in PAVEC following exposure to 100 ng/mL IL-6 and 5 μm Akt inhibitor XI. C) MEK1 expression was blocked in PAVEC following exposure to 100 ng/mL TNF-α and 25 μm PD98059 MEK1 inhibitor. Error bars show ±SEM, n ≥ 3 independent monolayers. Bars that do not share any letters are significantly different according to a one-way ANOVA with Tukey's post test ($p \leq 0.05$).

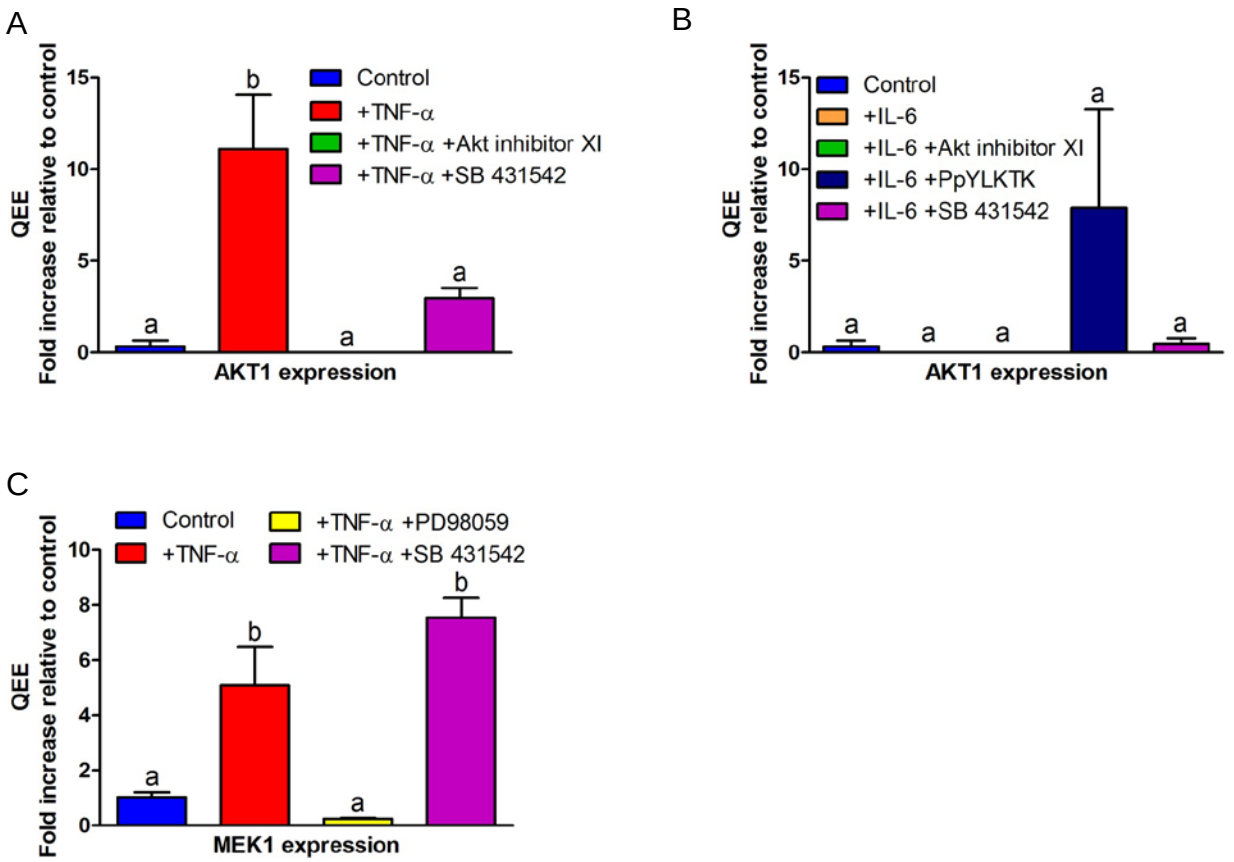

Figure XIII. AKT1 gene expression was blocked by Akt inhibition and MEK1 gene expression was blocked by MEK1 inhibition in QEE. A) AKT1 expression was blocked in QEE following exposure to 100 ng/mL TNF-α and 5 μm Akt inhibitor XI. B) AKT1 expression was blocked in QEE following exposure to 100 ng/mL IL-6 and 5 μm Akt inhibitor XI. C) MEK1 expression was blocked in QEE following exposure to 100 ng/mL TNF-α and 25 μm PD98059 MEK1 inhibitor. Error bars show ±SEM, n ≥ 3 batches of pooled explants. Bars that do not share any letters are significantly different according to a one-way ANOVA with Tukey's post test ($p \leq 0.05$).

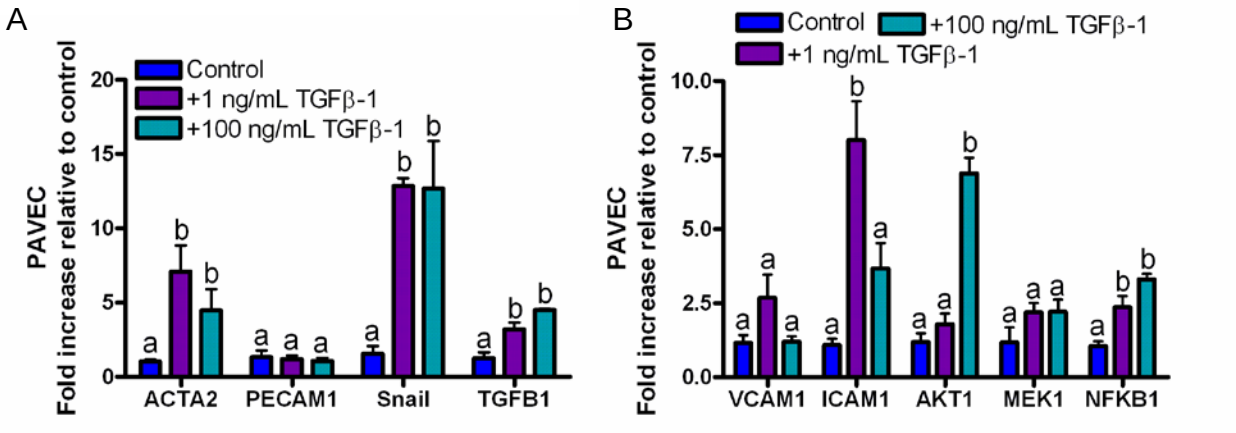

Figure XIV. EndMT related (A) and inflammatory activation-related (B) gene expression in porcine aortic valve endothelial cells (PAVEC) after exposure to 1 ng/mL or 100 ng/mL TGFβ-1. Error bars show ±SEM, n ≥ 3 independent monolayers. Bars that do not share any letters are significantly different according to a one-way ANOVA with Tukey's post test ($p \leq 0.05$).

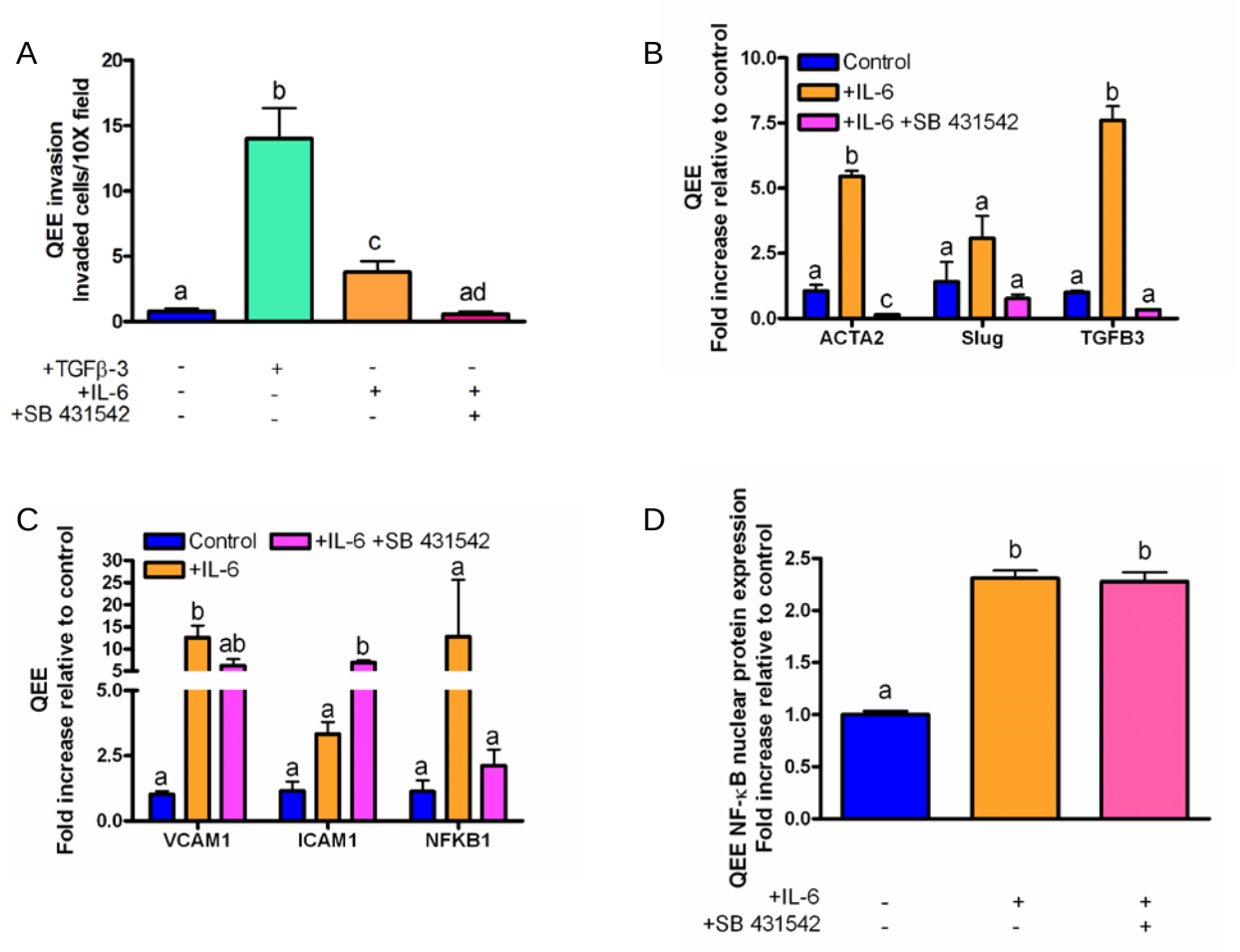

Figure XV. Embryonic endocardial monolayers co-opt TGFβ in inflammatory-EndMT signaling. A) Cell invasion after to exposure to 100 ng/mL TGFβ-3, 100 ng/mL IL-6, or 100 ng/mL IL-6 with 10 μm SB 431542 ALK5 inhibitor. B) EndMT-related gene expression after exposure to 100 ng/mL IL-6 with inhibitors. C) Inflammatory activation-related genes after exposure to 100 ng/mL IL-6 with inhibitors. D) QEE nuclear factor kappa b (NFκB) nuclear localization quantification after exposure to 100 ng/mL IL-6 with inhibitors. Error bars show ±SEM, n ≥ 3 batches of pooled explants. Bars that do not share any letters are significantly different according to a one-way ANOVA with Tukey's post test ($p \leq 0.05$).

References

1 Butcher JT, Penrod AM, Garcia AJ & Nerem RM. Unique morphology and focal adhesion development of valvular endothelial cells in static and fluid flow environments. *Arterioscler Thromb Vasc Biol*. 2004; 24: 1429-1434.

2 Simmons CA, Grant GR, Manduchi E & Davies PF. Spatial heterogeneity of endothelial phenotypes correlates with side-specific vulnerability to calcification in normal porcine aortic valves. *Circ Res*. 2005; 96: 792-799.

3 Guerraty MA, Grant GR, Karanian JW, Chiesa OA, Pritchard WF & Davies PF. Hypercholesterolemia induces side-specific phenotypic changes and peroxisome proliferator-activated receptor-g pathway activation in swine aortic valve endothelium. *Arterioscler Thromb Vasc Biol*. 2010; 30: 225-231.

4 Farivar RS, Cohn LH, Soltesz EG, Mihaljevic T, Rawn JD & Byrne JG. Transcriptional profiling and growth kinetics of endothelium reveals differences between cells derived from porcine aorta versus aortic valve. *Eur J Cardio-Thorac*. 2003; 24: 527-534.

5 Ku C-H, Johnson PH, Batten P, Sarathchandra P, Chambers RC, Taylor PM, Yacoub MH & Chester AH. Collagen synthesis by mesenchymal stem cells and aortic valve interstitial cells in response to mechanical stretch. *Cardiovasc Res*. 2006; 71: 548-556.

6 Osman L, Yacoub MH, Latif N, Amrani M & Chester AH. Role of human valve interstitial cells in valve calcification and their response to atorvastatin. *Circulation*. 2006; 114: I547-552.

7 Hafizi S, Taylor PM, Chester AH, Allen SP & Yacoub MH. Mitogenic and secretory responses of human valve interstitial cells to vasoactive agents. *J Heart Valve Dis*. 2000; 9: 454-458.

8 Holliday CJ, Ankeny RF, Jo H & Nerem RM. Discovery of shear- and side-specific mRNAs and miRNAs in human aortic valvular endothelial cells. *Am J Physiol Heart Circ Physiol*. 2011; 301: H856-867.

9 Moreland AF, Clarkson TB & Lofland HB. Atherosclerosis In "Miniature" Swine. I. Morphologic Aspects. *Arch Pathol*. 1963; 76: 203-210.

10 Skold BH, Getty R & Ramsey FK. Spontaneous atherosclerosis in the arterial system of aging swine. *Am J Vet Res*. 1966; 27: 257-273.

11 Swinkels DW & Demacker PNM. Comparative studies on the low density lipoprotein subfractions from pig and man. *Comp Biochem Phys B*. 1988; 90: 297-300.

12 Simmons CA, Grant GR, Manduchi E & Davies PF. Spatial heterogeneity of endothelial phenotypes correlates with side-specific vulnerability to calcification in normal porcine aortic valves. *Circ Res*. 2005; 96: 792-799.

13 de Smet BJGL, van der Zande J, van der Helm YJM, Kuntz RE, Borst C & Post MJ. The atherosclerotic Yucatan animal model to study the arterial response after balloon angioplasty: the natural history of remodeling. *Cardiovasc Res*. 1998; 39: 224-232.

14 Gerrity RG, Naito HK, Richardson M & Schwartz CJ. Dietary induced atherogenesis in swine: Morphology of the intima in prelesion stages. *Am J Pathol*. 1979; 95: 775–792.

15 Turk JR, Henderson KK, Vanvickle GD, Watkins J & Laughlin MH. Arterial endothelial function in a porcine model of early stage atherosclerotic vascular disease. *Int J Exp Pathol*. 2005; 86: 335-345.

16 Gould RA & Butcher JT. Isolation of valvular endothelial cells. *J Vis Exp.* 2010; 46: DOI: 10.3791/2158.

17 Schaffer CB, Friedman B, Nishimura N, Schroeder LF, Tsai PS, Ebner FF, Lyden PD & Kleinfeld D. Two-Photon Imaging of Cortical Surface Microvessels Reveals a Robust Redistribution in Blood Flow after Vascular Occlusion. *PLoS Biol*. 2006; 4: 0258 - 0270.

18 Yalcin H, Shekhar A, Rane A & Butcher J. An *ex-ovo* Chicken Embryo Culture System Suitable for Imaging and Microsurgery Applications. *J Vis Exp*. 2010; 44: DOI: 10.3791/2154.
19 Hinton RB, Jr., Lincoln J, Deutsch GH, Osinska H, Manning PB, Benson DW & Yutzey KE. Extracellular matrix remodeling and organization in developing and diseased aortic valves. *Circ Res*. 2006; 98: 1431-1438.
20 Wessels A & Sedmera D. Developmental anatomy of the heart: a tale of mice and man. *Physiol Genomics*. 2003; 15: 165-176.
21 Sedmera D, Cook AC, Shirali G & McQuinn TC. Current issues and perspectives in hypoplasia of the left heart. *Cardiol Young*. 2005; 15: 56-72.
22 Lincoln J, Alfieri CM & Yutzey KE. Development of heart valve leaflets and supporting apparatus in chicken and mouse embryos. *Dev Dyn*. 2004; 230: 239-250.
23 Mercado-Pimentel ME & Runyan RB. Multiple transforming growth factor-beta isoforms and receptors function during epithelial-mesenchymal cell transformation in the embryonic heart. *Cells Tissues Organs*. 2007; 185: 146-156.
24 Boyer AS, Ayerinskas, II, Vincent EB, McKinney LA, Weeks DL & Runyan RB. TGFbeta2 and TGFbeta3 have separate and sequential activities during epithelial-mesenchymal cell transformation in the embryonic heart. *Dev Biol*. 1999; 208: 530-545.
25 Hamburger V & Hamilton HL. A series of normal stages in the development of the chick embryo. *J Morphol*. 1951; **88**: 49-92.
26 Mahler GJ, Gould RA & Butcher JT. Isolation and culture of avian embryonic valvular progenitor cells. *J Vis Exp.* 2010; 44: DOI: 10.3791/2159.